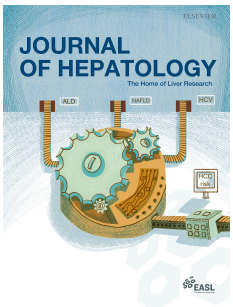

Prevalence, features and predictive factors of liver nodules in Fontan surgery patients: The VALDIG Fonliver prospective cohort

Luis Téllez, Enrique Rodríguez de Santiago, Beatriz Minguez, Audrey Payance, Ana Clemente, Anna Baiges, Dalia Morales-Arraez, Vincenzo La Mura, Elba Llop, Elena Garrido, Elvira Garrido-Lestache, Stephanie Tasayco, Onorina Bruno, Raquel Prieto, Silvia Montserrat, Mónica Pons, Andreína Olavarría, Laura Dos, Dominique Valla, María Jesús del Cerro, Rafael Bañares, Juan Carlos García-Pagán, Pierre-Emmanuel Rautou, Agustín Albillos, for the VALDIG an EASL consortium

PII: S0168-8278(19)30668-3

DOI: https://doi.org/10.1016/j.jhep.2019.10.027

Reference: JHEPAT 7532

To appear in: *Journal of Hepatology*

Received Date: 2 July 2019

Revised Date: 14 October 2019

Accepted Date: 30 October 2019

Please cite this article as: Téllez L, Rodríguez de Santiago E, Minguez B, Payance A, Clemente A, Baiges A, Morales-Arraez D, La Mura V, Llop E, Garrido E, Garrido-Lestache E, Tasayco S, Bruno O, Prieto R, Montserrat S, Pons M, Olavarría A, Dos L, Valla D, Jesús del Cerro M, Bañares R, García-Pagán JC, Rautou PE, Albillos A, for the VALDIG an EASL consortium, Prevalence, features and predictive factors of liver nodules in Fontan surgery patients: The VALDIG Fonliver prospective cohort, *Journal of Hepatology* (2019), doi: https://doi.org/10.1016/j.jhep.2019.10.027.

Liver nodules in Fontan-associated Liver Disease (FALD)

Liver nodules are frequent (47.7%)

Tipically: hyperechoic, hypervascular, peripheral

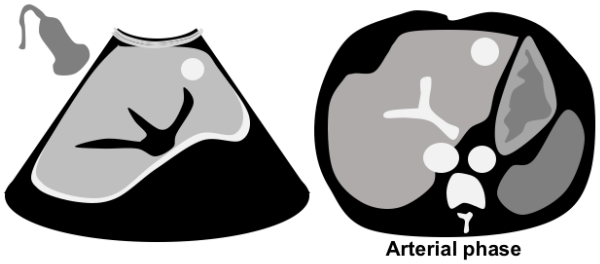

Arterial phase

Prevalence of HCC: 1.3%

Liver biopsy is mandatory to confirm HCC

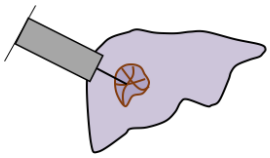

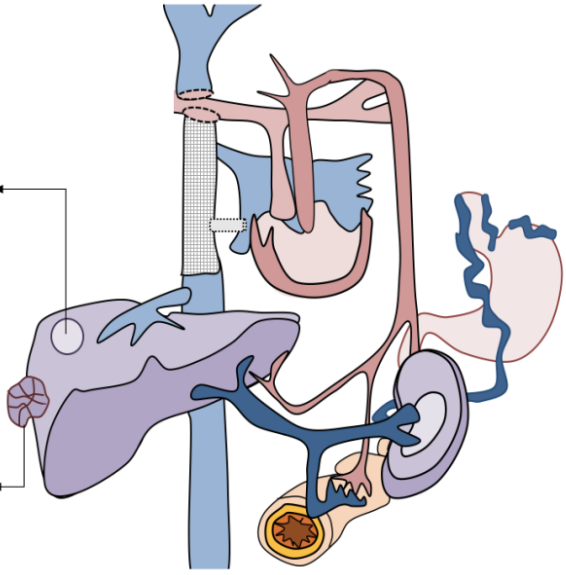

Title:

Prevalence, features and predictive factors of liver nodules in Fontan surgery patients: The VALDIG Fonliver prospective cohort

Authors

Luis Téllez[1]*, Enrique Rodríguez de Santiago[1]*, Beatriz Minguez[2], Audrey Payance[3], Ana Clemente[4], Anna Baiges[5] , Dalia Morales-Arraez[6], Vincenzo La Mura[7], Elba Llop[8], Elena Garrido[1], Elvira Garrido-Lestache[9], Stephanie Tasayco[2], Onorina Bruno[10], Raquel Prieto[11], Silvia Montserrat[12], Mónica Pons[2], Andreína Olavarría[13], Laura Dos[14], Dominique Valla[3], María Jesús del Cerro[9], Rafael Bañares[4], Juan Carlos García-Pagán[5], Pierre-Emmanuel Rautou[3], Agustín Albillos[1] for the VALDIG an EASL consortium.

* These authors share first authorship

Collaborators: Lara Aguilera, Rut Romera, Diego Rincón, María Álvarez Fuente, Xavier Merino, Massimo Chessa, Michela Triolo, Maxime Ronot, Valérie Vilgrain, Antoine Legendre, Caroline Chassing, Virginia Hernández-Gea; Maria Angeles Garcia-Criado; Anna Darnell, Ernest Belmonte, Fanny Turon, Jose Ferrusquia, Marta Magaz

Affiliations

1. Servicio de Gastroenterología y Hepatología, Hospital Universitario Ramón y Cajal, IRYCIS, CIBERehd, Universidad de Alcalá, Madrid, Spain.

2. Liver Unit, Department of Internal Medicine, Hospital Universitari Vall d'Hebron, Vall d'Hebron Institut of Research, CIBERehd, Universitat Autonoma de Barcelona, Barcelona, Spain.

3. Service d'Hépatologie, DHU Unity, Pôle des Maladies de l'Appareil Digestif, Hôpital Beaujon, AP-HP, Clichy, France.

4. Liver Unit, Hospital General Universitario Gregorio Marañón, Instituto de Investigación Sanitaria Gregorio Marañón, CIBERehd, Universidad Complutense, Madrid, Spain.

5. Barcelona Hepatic Hemodynamic lab, Liver Unit, Hospital Clínic, IDIBAPS, CIBERehd, Universidad de Barcelona, Barcelona, Spain.

6. Gastroenterology Department, University Hospital of the Canary Islands, La Laguna, Tenerife, Spain.

7. Fondazione IRCCS Ca' Granda, Ospedale Maggiore Policlinico, U.O.C. Medicina Generale Emostasi e Trombosi, C.R.C. "A.M. e A. Migliavacca" per lo Studio e la Cura

delle Malattie del Fegato and Dipartimento di Scienze Biomediche per la Salute, Università degli studi di Milano, Milano, Italy.

8. Servicio de Gastroenterología y Hepatología, Hospital Universitario Puerta de Hierro, Instituto de Investigación Sanitaria Puerta de Hierro, CIBERehd, Universidad Autónoma de Madrid, Madrid, Spain.

9. Servicio de Cardiología Infantil, Hospital Universitario Ramón y Cajal, IRYCIS, Universidad de Alcalá, Madrid, Spain.

10. Department of Radiology, APHP, University Hospitals Paris Nord Val de Seine, Beaujon, Clichy, Hauts-de-Seine, France.

11. Department of Cardiology, Hospital General Universitario Gregorio Marañón, Instituto de Investigación Sanitaria Gregorio Marañón, CIBERCV, Universidad Complutense, Madrid, Spain.

12. Institut Clínic Cardio-Vascular (ICCV), Hospital Clínic, Universitat de Barcelona, Catalonia, Spain; Institut d'Investigacions Biomèdiques August Pi i Sunyer (IDIBAPS), Barcelona, Catalonia, Spain; Centro de Investigacíon Biomédica en Red Enfermedades Cardiovasculares (CIBERCV), Madrid, Spain.
13. Servicio de Radiodiagnóstico, Hospital Universitario Ramón y Cajal, Madrid, Spain.

14. Unitat Integrada de Cardiopaties Congènites de l'Adolescent i de l'Adult Vall d'Hebron-Sant Pau. Se Hospital Universitario Vall d´Hebron. Barcelona

Corresponding author

Agustín Albillos, Servicio de Gastroenterología y Hepatología, Hospital Universitario Ramón y Cajal, Ctra Colmenar Viejo Km 9.100, 28034, Madrid, Spain.

Phone: +34 91368000 Email: agustin.albillos@uah.es

Financial support

Supported by grant from the Spanish Ministry of Science and Innovation (SAF 2017-86343-R to A.A.). CIBERHED is funded by the Instituto de Salud Carlos III with grants cofinanced by the European Development Regional Fund “A way to achieve Europe” (ERDF).

Authors contribution:

LT, ERS, AA- data acquisition, drafting of manuscript, interpretation of data, study concept. BM, AP, AB, DMA, VLM, EL, EG, EGL, ST, ON, RP, SM, MP, AO, LD- data acquisition and critical review of manuscript. DV, MJC, RB, JCGP, PER- preparation and critical review of manuscript.

Conflict of interest

The authors have no conflicts of interest that pertain to this work.

Electronic word count: 5848 words.

Number of figures: 1

Number of tables: 5

Lay summary

Fontan surgery is the standard of care for many patients with univentricular congenital cardiopathies. Recent advances have improved the survival of Fontan patients, and nowadays most of them reach adulthood. In this setting, Fontan-associated liver disease has been increasingly recognized, and has become a significant prognostic factor. Liver nodules are considered a component of FALD yet their prevalence, imaging features and predictors have hardly been evaluated in large patient series. In this multicentric study, we prospectively assessed liver nodules in a large number of Fontan patients. This allowed us to conclude that liver nodules are frequent, typically hyperechoic, hypervascular and predominantly peripheral. The risk of hepatocellular carcinoma is present, and biopsy is required for its diagnosis.

Highlights

- Liver nodules are frequent in Fontan patients.
- Some liver nodules may go unnoticed on abdominal ultrasound.
- The risk of hepatocellular carcinoma is low but present.
- Arterial hyperenhacement and washout are not specific of hepatocellular carcinoma in this population. Benign nodules may present arterial hyperenhacement and washout.
- Hepatocellular carcinoma in Fontan patients presents with suspicious radiological features and elevated alpha-fetoprotein.

ABSTRACT (261 words)

Background and aims: Fontan surgery is used to treat a variety of congenital heart malformations, and may lead to advanced chronic liver disease in the long-term. This study examines the prevalence, characteristics and predictors of liver nodules in patients with Fontan surgery.

Methods: This was a prospective, cross-sectional and observational study conducted at eight European centres. Consecutive patients with Fontan surgery underwent blood tests, abdominal ultrasonography (US), transient elastography (Fibroscan®), echocardiography, hemodynamics, and abdominal MRI/CT scan. The primary outcome measure was liver nodules detected in the MRI/CT scan. Predictors of liver nodules were identified by multivariate logistic regression.

Results: One hundred and fifty-two patients were enrolled (mean age 27.3 years). The mean time elapsed from surgery to inclusion was 18.3 years. Liver nodule prevalences were 29.6% (95% CI: 23–37%) on US and 47.7% (95% CI: 39-56%) on MRI/CT. Nodules were usually hyperechoic (76.5%), round-shaped (>80%), hyperenhancing in the arterial phase (92%) and located in the liver periphery (75%). The sensitivity and specificity of US were 50% (95% CI: 38-62%) and 85.3% (95% CI: 75-92%), respectively. Inter-imaging test agreement was low (adjusted kappa: 0.34). In the multivariate analysis, time since surgery > 10 years was the single independent predictor of liver nodules (OR: 4.18, P=0.040). Hepatocellular carcinoma was histologically diagnosed in 2 of the 8 patients with hypervascular and washout liver nodules.

Conclusion: While liver nodules are frequent in Fontan patients, they may go unnoticed in US. Liver nodules are usually hyperechoic, hypervascular and predominantly

peripheral. This population is at risk of hepatocellular carcinoma, the diagnosis of which requires biopsy confirmation.

Keywords: Fontan, heart, liver cirrhosis, liver nodules, hepatocellular carcinoma

INTRODUCTION

Fontan surgery (FS) is the standard of care for many patients with congenital cardiopathies characterised by a functionally univentricular heart. The common feature of these cardiac defects is the mixing of desaturated blood from the caval veins and oxygenated blood from the pulmonary veins in a single ventricular pump. Fontan circulation is a palliative strategy that aims to restore a double circulation system to avoid cyanosis. Improvements in surgical techniques and medical management have had a significant impact on survival, and nowadays most Fontan patients survive into adulthood [1,2]. However, systemic venous congestion and reduced systemic cardiac output are the hallmarks of FS, leading to long-term multiorgan complications [3,4]. Further, this single haemodynamic system in Fontan patients puts the liver at risk of vascular damage and advanced chronic liver disease.

Studies have shown that Fontan-associated liver disease (FALD) is an independent prognostic factor with a significant impact on survival [5]. Several retrospective single-centre studies with a limited sample size have also suggested that regenerative and hypervascular nodules on arterial phase imaging are frequent in this population [5–8]. As for other vascular liver diseases such as Budd-Chiari syndrome (BCS), the diagnosis of liver nodules (LN) in FALD is a significant challenge, since features and risk factors for their presence are poorly documented. Besides, the findings of several recent small case series have raised concerns about the risk of hepatocellular carcinoma in Fontan patients [9–11]. The American College of Cardiology statement on FALD underlines the need for periodic radiologic liver assessment, although evidence-supported recommendations are lacking [12].

To our knowledge, the present study is the first prospective multicentre investigation designed to assess the prevalence, characteristics, and predictor factors of

LN on cross-sectional imaging. As secondary objectives, we also addressed the diagnostic accuracy of abdominal ultrasonography (US) and inter-test agreement between US and MRI/CT in the Fontan population.

MATERIAL AND METHODS

Study design

This was an observational, prospective, cross-sectional study conducted at eight European tertiary centres belonging to the VALDIG group (ww.valdig.eu). All consecutive patients with FS were invited to participate in the study. No exclusion criteria were applied. The study period was December 2015 to October 2018. The study protocol adhered to the principles of the Declaration of Helsinki and was approved by the Ethics Committees for Clinical Research of all the participating institutions (IRB code: 384/14, HRC-FONLIVER). Written Informed consent for inclusion in the study was obtained in all cases.

Procedures and variables

A common standardized protocol was elaborated for the assessment of FALD before the study outset. Patients were subjected to a structured medical interview, physical examination, blood tests to rule out other liver disease etiologies, abdominal US, liver elastography (Fibroscan®, Probe M/XL Echosens®, Paris France), abdominal magnetic resonance imaging (MRI) or computed tomography (CT) when MRI was contraindicated, and echocardiography. Biopsy was considered by the multidisciplinary team in charge in patients with LN highly suspicious for malignancy as defined by i) arterial hyperenhancement and washout, ii) arterial hyperenhancement and enhancing capsule, iii) arterial hyperenhancement and > 20 mm, iv) hypo/iso-enhancement and >20 mm/enhancing capsule/washout. Due to the observational design of the study, a

haemodynamic evaluation was performed only when clinically indicated as deemed by the multidisciplinary team in charge. In every patient, all laboratory and imaging studies were performed within 6 months of inclusion in the study.

Baseline characteristics and blood tests

The demographic (age and sex) and clinical data compiled were: type of congenital heart defect, FS surgical technique [atriopulmonary, lateral tunnel or extracardiac], New York Heart Association functional classification (NYHA), time since FS, height, weight, body mass index, alcohol abuse defined as >20 g/day in women and >30 g/day in men, and blood pressure. The following laboratory parameters were assessed: serum creatinine, total bilirubin, alanine aminotransferase, aspartate aminotransferase, gamma-glutamyl transferase (GGT), alkaline phosphatase, C-reactive protein, brain natriuretic peptide, serology (Ig HAV, HBV, HCV, and HIV), ferritin, transferrin, serum copper, ceruloplasmin, alpha-1-antitrypsin, alpha-fetoprotein, albumin, immunoglobulins, total serum proteins, haemogram, and international normalised ratio.

Abdominal ultrasonography and liver elastography

Fasting for at least 8 hours was required for both procedures. US was performed by a radiologist or a hepatologist with expertise in abdominal imaging (>10,000 abdominal US)**.** The following variables were assessed: a nodular liver surface appearance, parenchymal echogenicity (homogeneous or heterogeneous), right hepatic lobe size in the longitudinal axis, central suprahepatic vein diameter, long spleen axis, ascites (absence, minimal or moderate-severe), presence of gallstones, and number and characteristics of LN. These characteristics included their size (defined as the longest cross-sectional diameter), echogenicity (hypoechoic, isoechoic, or hyperechoic), shape

(round, ellipsoidal or irregular with unclear margins) and peripheral location (outer margins within 2 cm of the liver border).

Liver elastography (Fibroscan®) was carried out by a trained operator (>1,000 procedures) blinded to patient clinical history. In all cases, at least ten measurements were obtained. Only when there were more than ten valid measurements and an interquartile range < 30 were considered valid. The final result was drawn from an average value expressed in kilopascals (kPa).

Abdominal MRI and CT scan

MRI and CT protocols are provided in **Supplementary material**. The following characteristics of the nodules were systematically assessed: size (defined as the longest cross-sectional diameter), peripheral location using the definition described above, arterial phase enhancement, shape (round, ellipsoidal or irregular), washout in the portal venous phase defined as hypointensity or hypodensity in part of, or in the whole lesion, on the portal venous and/or delayed phase compared to the surrounding liver parenchyma. We prospectively explored the behaviour of MRI/CT LI-RADS classification version 2014 [13]. Histological diagnosis of all biopsied nodules was recorded.

Cardiovascular assessment

Left ventricle ejection fraction was estimated by transthoracic echocardiography performed by cardiologists with expertise in congenital heart disease. The following parameters were recorded in the haemodynamic study: mean pulmonary artery pressure, inferior vena cava pressure, cardiac index calculated by Fick formula ($L/min/m^2$), hepatic vein pressure, hepatic vein wedge pressure, and hepatic vein pressure gradient. When a prospective haemodynamic evaluation was not performed, haemodynamic data

were retrieved from the previous year if the patient had not undergone major cardiac surgery.

Statistical analysis and sample size estimation

Quantitative variables are expressed as mean and standard deviation (SD) or median and range when these were non-normally distributed. Normality was tested through distributional graphs and the Shapiro-Wilk test. Frequency counts and percentages were used for categorical data. 95% confidence intervals (CI) for proportions were calculated by the Wilson method. Continuous variables were tested using parametric (t-test) and nonparametric tests (Mann-Whitney U test) when appropriate. Chi-squared and Fisher's exact tests were used for categorical data. Predictors of the presence of LN (any type of LN and LI-RADS ≥ 3) on MRI/CT were assessed by univariate and multivariate analysis. Variables found to be significant ($P < 0.1$) in the univariate analysis were entered in a multivariable binomial logistic regression through backward stepwise modelling. Time since surgery was entered as a binary variable (≤ 10 vs > 10 years) in the logistic model to meet the assumption that independent variables must be linearly related to the logit of the outcome. This time threshold was based on previous position statements on FALD [12].

Based on previous reports, we assumed a prevalence of LN of 40% on MRI/CT [14]. Assuming an α value of 0.05, attrition rate of 5%, and an absolute error of 8%, our initial sample size estimation was 153. For multivariate analyses, the rule of a minimum of ten events per variable was used [15].

Sensitivity, specificity, likelihood ratios and predictive values of abdominal US for the diagnosis of LN (any type of LN and LI-RADS ≥ 3) were calculated, setting MRI/CT scan as the reference technique. Inter-test agreement between US and MRI/CT was calculated via the prevalence-adjusted and bias-adjusted kappa statistic [16].

The following post-hoc univariate comparisons were performed to identify the reason for the low sensitivity of US found in the primary analysis: (1) LN seen on MRI/CT and not detected on US vs. LN seen on US and MRI/CT, (2) LN seen on US and not confirmed by MRI/CT vs LN seen on US and MRI/CT and (3) to address the possibility of a selection bias, we assessed any difference in results between patients who underwent all planned imaging procedures (n = 130) and the initial study population (n =152). Finally, an exploratory analysis was performed to assess whether the presence of two or more imaging signs of advanced chronic liver disease (blunt liver margin, heterogeneous liver parenchyma, portal vein > 13 mm, ascites or spleen long axis > 13 cm) were more common in patients with LN.

All tests were two-tailed. Significance was set at $P < 0.05$. Data were analyzed at the promoting institution (Hospital Universitario Ramón y Cajal, Madrid) using STATA software version 14.1 (StataCorp. Texas, USA).

RESULTS

Study population

The number of patients enrolled was 152 (**Figure 1, study flowchart**). Mean age was 27.3 years (SD: 7.8); 83 were male (54.6%). The most common congenital heart defects treated with FS were tricuspid atresia (44.7%), double inlet left ventricle (22.4%) and pulmonary atresia (13.2%). The mean time from FS to inclusion was 18.3 years (SD: 7.6). Extracardiac connection was the most frequent surgical procedure (64.5%). Although in 39 (25.7%) patients ejection fraction was below the normal range, the mean value in the whole cohort (56%) was within the normal limits (55 - 70%).

Total bilirubin, transaminases, alpha-fetoprotein, C-reactive protein, and albumin were within the normal range; while mean GGT (100 IU/ml) was slightly increased. Seven patients (4.6%) showed elevated alpha-fetoprotein (normal range: 0 –

8 IU/mL), which was above 15 IU/mL in only two patients, who were subsequently diagnosed with hepatocellular carcinoma. Four patients were diagnosed with chronic HCV infection and one patient had previously achieved a sustained virologic response with antiviral treatment. Mean liver stiffness was 26.1 kPa (SD: 15.1). Hemodynamic data were available from 66 patients. Mean hepatic venous pressure gradient was 2 mmHg (SD: 1.2, range: 0 – 6). Additional baseline characteristics are provided in **Table 1.**

Abdominal ultrasonography

The prevalence of patients with LN on US was 29.6% (45/152; 95% CI: 22.9 – 37.3%). The median number of nodules per patient was 2 and mean nodule size was 11 mm. Nodules were usually round (83.3%), hyperechoic (76.5%), and peripherally located in the liver (66.6%). Heterogeneous echogenicity (69.7%) and liver surface nodularity (54%) were frequent. Mean portal (10.2 mm) and central hepatic (8.9 mm) vein diameters were normal. Ascites was present in 29 patients (19.2%). Additional US findings are summarised in **Table 2**.

MRI and CT

Of the initial study population (n = 152), 130 patients underwent MRI (n = 93) or CT (n = 37). Nine patients refused MRI/CT; in 3 patients an MRI or CT scan was not deemed appropriate by the physician in charge due to poor heart functional status; and ten patients did not adhere to the protocol (in 3 patients > 6 months had elapsed between US and MRI/CT and 7 did not attend the scheduled visits for cross-sectional imaging). Demographic and clinical variables and LN prevalences and features were similar in patients that did or did not comply with the established protocol (**Supplementary Table 1**).

A higher prevalence of LN was detected on MRI/CT than on abdominal US (62/130, 47.7%; 95% CI: 39.3 - 56.2%) amounting to a total of 173 nodules of median size 9 mm. Nodules were often hyperenhancing in the arterial phase (92.3%), round (90.3%), and peripherally located (74.8%). When the LI-RADS classification was applied, LI-RADS-3 nodules (59.4%) were the most frequent type. Eleven LN (7.1%) showed washout. Additional nodule characteristics on MRI/CT are provided in **Table 3.**

In the univariate analysis, symptomatic protein-losing enteropathy (p = 0.026) and time since FS > 10 years (p = 0.037) were associated with the presence of LN **(Table 4)**. In the logistic regression, only the latter remained as a significant predictor of any type of LN (FS > 10 years OR = 4.18, 95% CI: 1.07 – 16.4; P = 0.040). Additionally, in the exploratory analysis, time since FS > 10 years was also the single predictor of LI-RADS ≥ 3 LN (OR = 4.23, 95% CI: 1.03 – 17.6; P = 0.046) (**Supplementary Table 2)**. The number of patients with nodules paralleled the number of years elapsed from FS (**Supplementary Table 3).**

Summary of sensitivity, specificity and predictive values

The sensitivity of US for the diagnosis of LN was 50% (95% CI: 37.9 - 62.1%) and specificity 85.3% (95% CI: 75 - 91.8%). Global accuracy was 68.5% (95% CI: 60 – 75.8%).

For tests restricted to the detection of LI-RADS ≥ 3 LN, sensitivity was 56% (95% CI: 42.3 - 68.8%) and specificity 83.8% (95% CI: 74.2 – 90.3%). Global accuracy was 73.1% (95% CI: 64.9 - 80%). Predictive values and likelihood ratios are provided in **Supplementary Table 4**

Patients with liver nodules highly suspicious of malignancy

Table 5 describes the characteristics of the 8 patients (8/130, 6.1%) with LN highly suspicious of malignancy (i.e. LI-RADS 4-5) on cross-sectional imaging. US did not identify the LN in 2 of these 8 patients. Biopsy of LN was undertaken on 7 of these 8 patients and showed hepatocellular carcinoma in 2 patients, and absence of malignancy in the other 5 (prevalence of hepatocellular carcinoma 1.3%). The hepatocellular carcinoma nodules were isoechoic on US and patients had elevated alpha-fetoprotein (272 and 339 IU/mL). One of these 2 patients had serologic features of spontaneous clearance of HCV infection (antiHCV+, HCV-RNA –) and had not received antiviral therapy; while the other lacked additional etiological factors of chronic liver disease. Finally, a patient with a 17 mm LN hypervascular and with washout, and with normal serum alfa-fetoprotein refused to undergo biopsy. The LN of the latter patient has remained unchanged in 3- 6- and 12-month CT scans.

Inter-test agreement and post-hoc analyses of liver nodules

Inter-test US vs. MRI/CT agreement was low (prevalence-adjusted and bias-adjusted kappa statistic = 0.34). In ten patients, LN seen on US were not confirmed in the MRI/CT scan. These lesions were smaller (median size: 0.6 mm, P = 0.036) and more often hyperechoic (95.7%, P = 0.038) than LN detected with both imaging techniques (**Supplementary Table 5**).

In 31 out of 62 patients in whom LN were seen in the MRI/CT scan, US did not detect any lesion. LN exclusively detected on MRI/CT were more often hypervascular (96.6%, P = 0.03) than those identified with both imaging techniques (86.6%). No further significant differences were found (**Supplementary Table 5**). Interestingly, LN with biopsy-proven hepatocellular carcinoma were detected by CT/MRI and US.

The presence of ≥2 imaging signs of advanced chronic liver disease did not predict the presence of LN (P = 0.23) on US or MRI/CT (P = 0.74) (**Supplementary Table 6**)

DISCUSSION

This study prospectively examines the prevalence and imaging features of LN in a large series of Fontan patients. Our findings indicate that i) LN are common and their frequency increases in parallel to the time elapsed since Fontan surgery, ii) US shows a rather low sensitivity to identify LN, iii) most of these nodules show hypervascular behaviour on CT/MRI but result on non-neoplastic regenerative hepatocytes, and iv) hepatocellular carcinoma is a possibility, albeit unlikely.

Liver nodules were detected in approximately half of the study participants. Reported prevalences of LN in patients with FALD have been lower, ranging from 17 to 40% [7,8,14,17,18]. The higher prevalence detected here could be explained by the exclusive use of US or the retrospective and non-systematic assessment of LN in previous studies. In addition, our cohort showed a higher mean time since FS, which is a known risk factor for advanced chronic liver disease and hepatic complications [5,12,19,20].

Upon US, we observed that LN were commonly hyperechoic, < 2 cm, multiple, and located in the periphery of the liver, in line with the findings of US studies

conducted on smaller samples [17,21]. Some nodules, especially when small (< 1 cm) and hyperechoic, were not reproduced in the MRI/CT scan. According to some authors, some of these LN exclusively visible on US examination could represent small areas with microvascular disturbances or early-stage fibrosis [17]. As expected, additional signs suggestive of liver disease such as liver contour nodularity, heterogeneous parenchyma and ascites were commonly encountered. Interestingly, our results show that classical imaging signs of advanced chronic liver disease do not predict the presence of LN.

One of our main findings was that the sensitivity of US for the diagnosis of LN was low. This could be because US is more operator-dependent than MRI/CT scanning and the vascular nature of LN in FALD. Actually, some lesions were only seen in the arterial phase after contrast injection and arterial hyperenhancement was more common in LN that were not detected by US. In a recent study examining 49 Fontan patients, it was found that LN were missed on US in approximately 30% of cases [8]. Taken together, these observations suggest that contrast-enhanced modalities may be more suitable to identify the full spectrum of LN in patients with FALD. US did not detect any LN in two patients with LI-RADS 5 lesions, but very importantly did not miss any case of hepatocellular carcinoma in our cohort and, consequently, we cannot conclude from our data that this imaging modality should be ruled out as a screening tool. To date, only one study has assessed the benefits of surveillance imaging in FALD [22]. Because of the retrospective design and heterogeneity of intervals and imaging techniques in this study, the authors could only recommend surveillance. However, the optimal management strategy for these patients remains to be established.

A high risk of hepatocellular carcinoma is a major concern and this is what prompted our study. However, despite the high prevalence of LN in our FS cohort, the

proportion of malignant LN was low. Post-mortem series and biopsy studies have shown that most LN correspond to focal nodular hyperplasia (FNH) or benign regenerative nodules [6,7,18,21,23]. FNH is a polyclonal lesion occurring in the setting of normal parenchyma and has been linked to a hyperplastic response to increased blood flow induced by a focal vascular abnormality [24]. As shown here, hepatic adenoma may also appear after FS and there have been some case reports in FALD [23]. Adenoma underdiagnosis is a possibility, as these may resemble FNH-like lesions in terms of size, imaging and histological features [25]. In some of our patients with biopsy-proven non-malignant lesions washout features were found. Interestingly, a low specificity of washout to diagnose hepatocellular carcinoma has been also recently described in a French cohort of patients with BCS [26]. In another recent study, it was shown that benign hyperenhancing nodules detected after FS may display washout and be mistaken for hepatocellular carcinoma according to imaging criteria [18]. As shown in our two patients with hepatocellular carcinoma, alpha-fetoprotein is usually elevated in cases of malignancy, as occurs in BCS [10,11,27,28]. Based on our results, we would argue that the hepatocellular carcinoma diagnostic criteria used in cirrhosis are not applicable in FALD, and biopsy confirmation is always required [9,18,23].

The origin of LN has been linked to perfusion disturbances in the liver parenchyma secondary to Fontan circulation, similar to the nodules encountered in BCS and other vascular liver diseases [6,7,18,24]. It should be noted that extrapolating data from BCS and other forms of liver cirrhosis may be inaccurate, since the portal hypertension model in FALD is characteristically hypodynamic and arterial splanchnic perfusion may also be impaired, as shown in Doppler studies [29]. In fact, this is what makes FALD a unique entity. Some authors propose that impaired hepatic venous outflow caused by elevated right central pressures leads to atrophy and hypoxia-induced

damage, followed by a compensatory mechanism characterised by the arterialisation of liver parenchyma and regenerative changes [7,14]. Elevated right pressures and liver stiffness have also been described as potential markers of LN in univariate analyses of previous studies, but these results were not reproduced here [7,8]. Inflammation and cholestatic-induced injury are thought to play a minor role in LN and FALD progression [5,7,23]. In contrast, we identified time since FS > 10 years as a predictive factor for LN. This is an important finding providing further support for the expert-based consensus that liver assessment is mandatory 10 years after FS [30].

Our study has some limitations. First, it could be argued that some lesions that were not biopsied could harbour hepatocellular carcinoma. However, available data suggest that hepatocellular carcinoma in FALD usually presents with suspicious radiological features (i.e. hyperenhancing nodules with washout) or elevated alpha-fetoprotein. Moreover, liver biopsy in patients with elevated systemic pressures who are frequently under antithrombotic treatment carries a significant risk of adverse events. Considering that all but one patient with LN showing worrisome features underwent biopsy, we believe that the risk of underdiagnosed hepatocellular carcinoma is likely to be low. Secondly, some patients did not undergo the same cross-sectional imaging. CT scanning was reserved for patients in whom MRI was contraindicated to minimize radiation exposure in this young population. Further, according to a recent report, agreement between MRI and CT is high in the FALD setting (kappa statistic = 0.85) [8]. Third, LI-RADS classification has been developed to standardise the reporting of LN in patients with cirrhosis, but it has not been validated in patients with FALD. Therefore, the LI-RADS sub-analysis in our series should be regarded as merely exploratory, since the absence of validation of LI-RADS criteria in FALD precludes its application in this population. Finally, our study design precluded any assessment of the natural history of

LN in the long-term. We anticipate that further longitudinal study of this cohort will shed some light on this issue.

In conclusion, LN frequently appear in FALD and may not be detected in an US exam. These nodules are usually hyperechoic, hypervascular, mainly located in the liver periphery and are more often encountered later than ten years after FS. The risk of hepatocellular carcinoma is low but present, and its diagnosis requires biopsy confirmation.

References

[1] Poh CL, d'Udekem Y. Life After Surviving Fontan Surgery: A Meta-Analysis of the Incidence and Predictors of Late Death. Heart Lung Circ 2018;27:552–9.

[2] Dabal RJ, Kirklin JK, Kukreja M, Brown RN, Cleveland DC, Eddins MC, et al. The modern Fontan operation shows no increase in mortality out to 20 years: a new paradigm. J Thorac Cardiovasc Surg 2014;148:2517-2523.e1.

[3] Camposilvan S, Milanesi O, Stellin G, Pettenazzo A, Zancan L, D'Antiga L. Liver and cardiac function in the long term after Fontan operation. Ann Thorac Surg 2008;86:177–82.

[4] Gewillig M, Brown SC. The Fontan circulation after 45 years: update in physiology. Heart 2016;102:1081–6.

[5] Wu FM, Kogon B, Earing MG, Aboulhosn JA, Broberg CS, John AS, et al. Liver health in adults with Fontan circulation: A multicenter cross-sectional study. J Thorac Cardiovasc Surg 2017;153:656–64.

[6] Engelhardt EM, Trout AT, Sheridan RM, Veldtman GR, Dillman JR. Focal liver lesions following Fontan palliation of single ventricle physiology: A radiology-pathology case series. Congenit Heart Dis 2019;14:380-388.

[7] Bryant T, Ahmad Z, Millward-Sadler H, Burney K, Stedman B, Kendall T, et al. Arterialised hepatic nodules in the Fontan circulation: hepatico-cardiac interactions. Int J Cardiol 2011;151:268–72.

[8] Horvat N, Rocha MS, Chagas AL, Oliveira BC, Pacheco MP, Binotto MA, et al. Multimodality Screening of Hepatic Nodules in Patients With Congenital Heart Disease After Fontan Procedure: Role of Ultrasound, ARFI Elastography, CT, and MRI. AJR Am J Roentgenol 2018;211:1212–20.

[9] Asrani SK, Warnes CA, Kamath PS. Hepatocellular carcinoma after the Fontan procedure. N Engl J Med 2013;368:1756–7.

[10] Josephus Jitta D, Wagenaar LJ, Mulder BJM, Guichelaar M, Bouman D, van Melle JP. Three cases of hepatocellular carcinoma in Fontan patients: Review of the literature and suggestions for hepatic screening. Int J Cardiol 2016;206:21–6.

[11] Martínez-Quintana E, Monescillo A, Rodríguez-González F. Hepatocellular carcinoma in a non-failing Fontan circulation. Rev Esp Enferm Dig 2017;109:375.

[12] Daniels CJ, Bradley EA, Landzberg MJ, Aboulhosn J, Beekman RH, Book W, et al. Fontan-Associated Liver Disease: Proceedings from the American College of Cardiology Stakeholders Meeting, October 1 to 2, 2015, Washington DC. J Am Coll Cardiol 2017;70:3173–94.

[13] LI-RADS n.d. https://www.acr.org/Clinical-Resources/Reporting-and-Data-Systems/LI-RADS (accessed June 16, 2019).

[14] Wallihan DB, Podberesky DJ. Hepatic pathology after Fontan palliation: spectrum of imaging findings. Pediatr Radiol 2013;43:330–8.

[15] Vittinghoff E, McCulloch CE. Relaxing the rule of ten events per variable in logistic and Cox regression. Am J Epidemiol 2007;165:710–8.

[16] Mak HKF, Yau KKW, Chan BPL. Prevalence-adjusted bias-adjusted kappa values as additional indicators to measure observer agreement. Radiology 2004;232:302–3.

[17] Bae JM, Jeon TY, Kim JS, Kim S, Hwang SM, Yoo S-Y, et al. Fontan-associated liver disease: Spectrum of US findings. Eur J Radiol 2016;85:850–6.

[18] Wells ML, Hough DM, Fidler JL, Kamath PS, Poterucha JT, Venkatesh SK. Benign nodules in post-Fontan livers can show imaging features considered diagnostic for hepatocellular carcinoma. Abdom Radiol (NY) 2017;42:2623–31.

[19] Goldberg DJ, Surrey LF, Glatz AC, Dodds K, O'Byrne ML, Lin HC, et al. Hepatic Fibrosis Is Universal Following Fontan Operation, and Severity is Associated With Time From Surgery: A Liver Biopsy and Hemodynamic Study. J Am Heart Assoc 2017;6.
[20] Johnson JA, Cetta F, Graham RP, Smyrk TC, Driscoll DJ, Phillips SD, et al. Identifying predictors of hepatic disease in patients after the Fontan operation: a postmortem analysis. J Thorac Cardiovasc Surg 2013;146:140–5.
[21] Kim T-H, Yang HK, Jang H-J, Yoo S-J, Khalili K, Kim TK. Abdominal imaging findings in adult patients with Fontan circulation. Insights Imaging 2018;9:357–67.
[22] Nandwana SB, Olaiya B, Cox K, Sahu A, Mittal P. Abdominal Imaging Surveillance in Adult Patients After Fontan Procedure: Risk of Chronic Liver Disease and Hepatocellular Carcinoma. Curr Probl Diagn Radiol 2018;47:19-22.
[23] Ghaferi AA, Hutchins GM. Progression of liver pathology in patients undergoing the Fontan procedure: Chronic passive congestion, cardiac cirrhosis, hepatic adenoma, and hepatocellular carcinoma. J Thorac Cardiovasc Surg 2005;129:1348–52.
[24] Sempoux C, Balabaud C, Paradis V, Bioulac-Sage P. Hepatocellular nodules in vascular liver diseases. Virchows Arch 2018;473:33–44.
[25] Sempoux C, Paradis V, Komuta M, Wee A, Calderaro J, Balabaud C, et al. Hepatocellular nodules expressing markers of hepatocellular adenomas in Budd-Chiari syndrome and other rare hepatic vascular disorders. J Hepatol 2015;63:1173–80.
[26] van Wettere M, Purcell Y, Bruno O, Payancé A, Plessier A, Rautou P-E, et al. Low specificity of washout to diagnose hepatocellular carcinoma in nodules showing arterial hyperenhancement in patients with Budd-Chiari. J Hepatol 2019;70:1123-1132.
[27] Conroy MR, Moe TG. Hepatocellular carcinoma in the adult Fontan patient. Cardiol Young 2017;27:407–9.
[28] Egbe AC, Poterucha JT, Warnes CA, Connolly HM, Baskar S, Ginde S, et al. Hepatocellular Carcinoma After Fontan Operation. Circulation 2018;138:746–8.
[29] Kutty SS, Peng Q, Danford DA, Fletcher SE, Perry D, Talmon GA, et al. Increased hepatic stiffness as consequence of high hepatic afterload in the Fontan circulation: a vascular Doppler and elastography study. Hepatology 2014;59:251–60.
[30] Rychik J, Veldtman G, Rand E, Russo P, Rome JJ, Krok K, et al. The precarious state of the liver after a Fontan operation: summary of a multidisciplinary symposium. Pediatr Cardiol 2012;33:1001–12.

Table 1. Baseline characteristics

Number of patients	152
Age, years	27.3 (7.8)
Male sex	83 (54.6%)
Body mass index, kg/m^2	22.8 (4.1)
Protein-losing enteropathy	15 (9.9%)
Cardiologic and haemodynamic assessment	
Main congenital heart defect	
Tricuspid atresia	68 (44.7%)
Double inlet left ventricle	34 (22.4%)
Pulmonary atresia	20 (13.2%)
Complete AVSD	12 (7.9%)
Criss-cross ventricles	5 (3.3%)
Mitral valve atresia	4 (2.6%)
Other	9 (5.9%)
Type of Fontan connection	
Atriopulmonary	41 (27%)
Extracardiac	98 (64.5%)
Lateral tunnel	13 (8.5%)
Time since Fontan connection, years	18.3 (7.6)
Pacemaker	37 (24.3%)
Flutter/atrial fibrillation	29 (19.3%)
NYHA functional class	
I	83 (54.6%)
II	52 (34.2%)
III	14 (9.2%)
IV	3 (2%)
Systolic blood pressure, mmHg	113 (13)
Diastolic blood pressure, mmHg	69 (9)
Oxygen saturation, %	94 (3.2)
Ejection fraction on echocardiography, %	56 (7.8)
Haemodynamic study (n=66)	
Pulmonary artery medium pressure, mmHg	14.9 (3.9)
Inferior vena cava, mmHg	15.4 (3.7)
Cardiac index, L/min/m^2	3.3 (1.6)
Free Hepatic vein pressure, mmHg	15.5 (4.9)
Wedged Hepatic vein pressure, mmHg	17.5 (5.5)
Hepatic venous pressure gradient, mmHg	2 (1.2)
Treatment	
Antiaggregant	78 (51.3%)
Anticoagulant	67 (44.1%)
Beta-blocker	58 (38.2%)
Diuretic	35 (23%)
Sildenafil	14 (9.2%)
Amiodarone	5 (3.3%)
Liver assessment	
Alcohol consumption (>20-30 g/week)	12 (7.9%)
Laboratory	

Creatinine, mg/dL	0.79 (0.14)
Total bilirubin, mg/dL	1.3 (0.82)
Sodium, mmol/L	139.5 (2.6)
AST, IU/L	29 (13.3)
ALT, IU/L	31 (19.7)
Alkaline phosphatase, IU/L	97 (68)
Gamma-glutamyl transferase, IU/L	100 (65)
Albumin, g/dL	4.2 (0.7)
Total proteins, g/dL	7.2 (0.9)
BNP, pg/mL	108 (161)
Ig G, mg/dL	1,135 (349)
Ig A, mg/dL	113 (139)
Ig M, mg/dL	118 (64)
Anti-HIV	0
HBsAg	0
Anti-HCV	5 (3.3%)
HCV-RNA +	4 (2.6%)
Alpha-fetoprotein, IU/mL	2.5 (1.3 – 3.5)
C-reactive protein, mg/L	4.2 (5.2)
Platelet*10^3/mm^3	151 (60.5)
INR	1.5 (0.7)
MELD-XI	10.8 (2.1)
Liver stiffness (Fibroscan®), kPa	26.2 (15.1)

Quantitative variables are provided as means (standard deviation) or median (interquartile range). Qualitative variables are expressed as absolute values and percentages.

AVSD: atrioventricular septal defect, NYHA: New York Heart Association, ALT: alanine transaminase, AST: aspartate aminotransferase, BNP: brain natriuretic peptide, HBsAg: Hepatitis B surface antigen, HCV: Hepatitis C virus, MELD-XI: model for end-stage liver disease excluding INR.

Table 2. Ultrasonographic findings

Number of patients	152
Liver surface nodularity	82 (54%)
Heterogeneous echogenicity	106 (69.7%)
Righ hepatic lobe, cm	13 (1.9)
Portal vein diameter, mm	10.2 (2.5)
Central hepatic vein diameter, mm	8.9 (2.4)
Spleen diameter, cm	12.9 (2.5)
Splenomegaly (long axis > 13 cm)	72 (47.3%)
Ascites	
Minimal	23 (15.3%)
Moderate-severe	6 (3.9%)
Gallstones	26 (16.1%)
Patients with one or more hepatic nodules	
No. of patients	45 (29.6%)
Median no. of nodules per patient	2 (1-3)
Total no. of nodules *	102
Median size, mm	11 (6-18)
No. of patients with one or more nodules ≥ 1 cm	39 (25.6%)
Median size of the largest nodule, mm	14 (7-20)
Patients with a no. of nodules equal to	
1	15 (33.3%)
2	11 (24.4%)
3	10 (22.2%)
4	2 (4.4%)
7	1 (2.2%)
10	1
Nodular parenchyma with countless micronodules	5 (11.1%)
Echogenicity	
Hyperechoic	78 (76.5%)
Isoechoic	15 (14.7%)
Hypoechoic	5 (4.9%)
Unclassified	4 (3.9%)
Peripheral location	68 (66.6%)
Shape	
Round	85 (83.3%)
Ellipsoidal	7 (6.8%)
Irregular with unclear margins	5 (4.9%)
Unclassified	5

Quantitative variables are provided as means (standard deviation) or median (interquartile range). Qualitative variables are expressed as absolute values and percentages.

* Five patients with countless micronodules were excluded from the analysis of nodule characteristics.

Table 3. Hepatic nodules in patients undergoing MRI or CT

Number of patients	130
MRI	93
CT	37
Patients with one or more nodules	62 (47.7%)
Total number of nodules	173
No. of nodules per patient	0 (0-1)
Size, mm	9 (6-12)
Size of the largest nodule, mm	13 (10-21)
No. of patients with one or more nodules ≥ 1 cm	54 (41.5%)
Patients with a no. of nodules equal to	
1	30 (23.1%)
2	15 (11.5%)
3	6 (4.6%)
4	1 (0.8%)
5	2 (1.5%)
7	2
9	1
10	2
12	2
14	1
No. of nodules assessed for characteristics (n: 155) *	
Arterial phase enhancement	143 (92.3%)
Peripheral location	116 (74.8%)
Shape	
Round	140 (90.3%)
Ellipsoidal	6 (3.9%)
Irregular	9 (5.8%)
Washout	11 (7.1%)
LI-RADS	
1	10 (6.4%)
2	24 (15.5%)
3	92 (59.4%)
4	6 (3.9%)
5	5 (3.2%)
Unclassified	18 (11.6%)
MRI (No. of patients: 93, No. of nodules: 106)	
T1-weighted	
Hypointense	17 (16%)
Isointense	76 (71.7%)
Hyperintense	6 (5.7 %)
Unclassified	7 (6.6 %)
T2-weighted	
Hypointense	6 (5.7 %)
Isointense	85 (80.2%)
Hyperintense	8 (7.5%)
Unclassified	7 (6.6 %)

Quantitative variables are provided as means (standard deviation or median [interquartile range]). Qualitative variables are expressed as absolute values and percentages.

* In patients with more than seven nodules only those > 0.5 mm were characterised.

Table 4. Predictors of liver nodules on MRI or CT

Variable	Patients with nodules	Patients without nodules	Univariate P-values	Multivariate logistic regression Odds ratio (confidence interval 95%) P-value
Number of patients (n = 130)	62	68		
Age, years	27.1	29	0.16	
Male Sex	35 (56.4%)	36 (53%)	0.68	
Time Fontan connection > 10 years	59 (95.1%)	57 (83.8%)	**0.037**	**4.18 (1.07 – 16.4); P = 0.040**
Enteropathy	10 (16.1%)	3 (4.4%)	**0.026**	3.84 (0.98 – 14.9); P = 0.053
Body mass index	22.6	23.4	0.28	
Type of Fontan			0.44	
Atriopulmonary	15 (24.2%)	21 (30.9%)		
Extracardiac	43 (69.4%)	40 (58.8%)		
Lateral tunnel	4 (6.4%)	7 (10.3%)		
Bilirubin, mg/dL	1.4	1.3	0.28	
Alkaline phosphatase, IU/L	93	103	0.37	
Gamma-glutamyl transferase, IU/L	106	98	0.5	
Brain natriuretic peptide, pg/mL	83	123	0.21	
Alpha-fetoprotein, IU/mL	13.4	2.7	0.15	
Ventricle ejection fraction, %	57	55	0.19	
Haemodynamic (n = 66)				
Pulmonary artery medium pressure, mmHg	14.9	15.3	0.7	
Inferior vena cava, mmHg	15.7	15.5	0.88	
Cardiac index, L/min/m^2	3.5	3	0.29	
Liver stiffness, kPa	28	24.8	0.25	
Ascites in MRI/CT	13 (21%)	12 (17.5%)	0.63	

Quantitative variables are provided as means and qualitative variables as absolute values and percentages. Figures in bold indicate significance. kPa: kilopascals.

Table 5. Patients with liver nodules highly suspicious of malignancy

Sex and age (years)	Type of Fontan	Time since Fontan (years)	Liver stiffness (kPa)	Alfa-fetoprotein (IU/L)	US nodules	MRI/CT nodules	Histology	Management
Male 23.4	Extracardiac	17.7	55.2	4	No. 1: 17 mm round hyperechoic Nos. 2, 3: 6 mm round hyperechoic	No. 1: 22 mm, hypervascular, washout. LI-RADS 5 No. 2: 17 mm, hypervascular, washout. LI-RADS 4	Core biopsy nodule No.1: negative for malignancy	3-month imaging follow up
Female 38.3	Atriopulmonar	34.5	22.3	272	20 mm irregular and isoechoic	20 mm, hypervascular, washout. LI-RADS 5	Hepatocellular carcinoma	Radiofrequency
Male 33	Atriopulmonar	27.4	48	1.3	No. 1: 10 mm round hyperechoic No. 2: 6 mm round hyperechoic No. 3: 5 mm round hyperechoic	No. 1: 12 mm, hypervascular, washout. LI-RADS 4 No. 2: 3 mm, hypervascular, no washout. LI-RADS 3	Core biopsy nodule No.1: negative for malignancy	3-month imaging follow up
Male 17	Atriopulmonar	15.6	11.6	1	No	No. 1: 14 mm, hypervascular,	PAAF nodule no.1: inconclusive.	3-month imaging follow up

						washout, enhancing capsule. LI-RADS 5 No. 2: 11 mm, hypervascular, washout. LI-RADS 4 No. 3: 6 mm, hypervascular, no washout. LI-RADS 3	Core biopsy nodule No. 1: negative for malignancy	
Male 26	Atriopulmonar	19.2	70	339	No. 1: 40 mm round, Isoechoic No. 2: 18 mm round hypoechoic	No. 1: 40 mm, hypervascular, washout. LI-RADS 5 No. 2: 16 mm, hypervascular, washout. LI-RADS 4	Core biopsy nodule No. 1: Hepatocellular carcinoma	Chemoembolisation
Male 24	Extracardiac	11	12.5	1	3 hyperechoic nodules (21,15,7 mm)	No. 1: 15 mm, hypervascular, washout. LI-RADS 4 No. 2: 15 mm, isodense, LI-RADS 1	Core biopsy nodule No. 1: Adenoma	3-month imaging follow up
Male 37	Atriopulmonar	25	73.5	2	No	No. 1: 16 mm, hypervascular,	Core biopsy nodule No. 1: Adenoma	6-month imaging follow up

						washout, enhancing capsule. LI-RADS 5. No. 2: 3 mm, hypervascular, no washout, LI-RADS 3		
Female 23.5	Extracardiac	16.5	35.3	1.2	20 mm round hyperechoic	No. 1: 17 mm, hypervascular, washout. LI-RADS 4	Not performed	3- and 12-month imaging follow up

FIGURES

Figure 1. Study flowchart

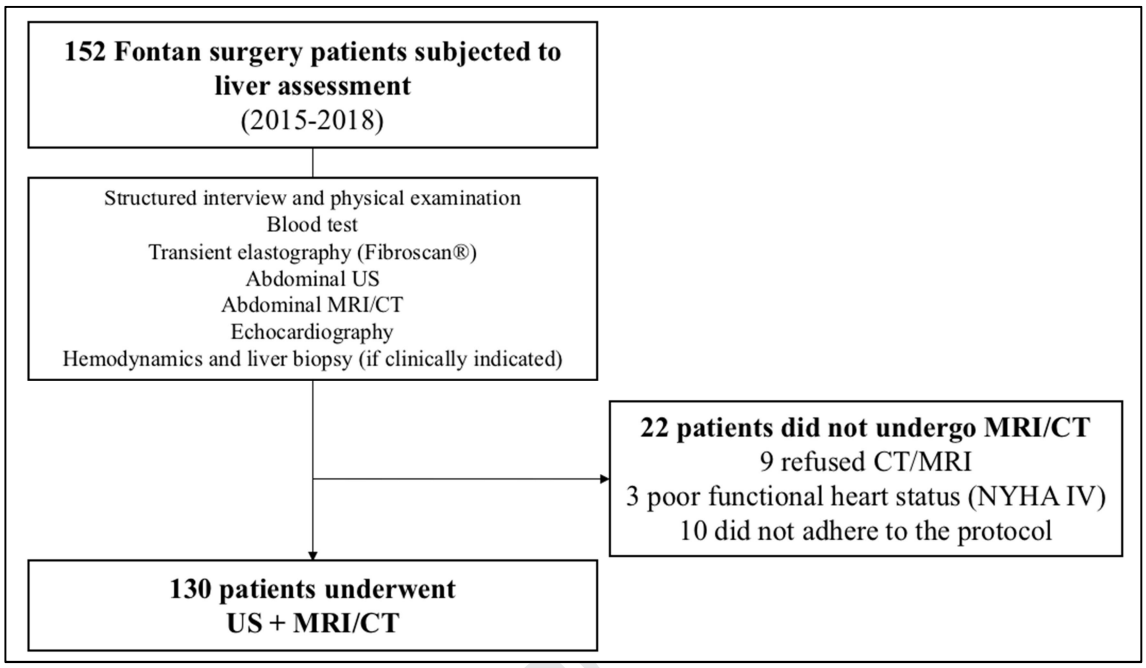

CT: computerised tomography; MRI: magnetic resonance imaging; NYHA: New York Heart Association; US: ultrasonography